PHYSICS AND CHEMISTRY OF SOLID STATE
V. 22, No. 4 (2021) pp. 828-836
Section: Technology

DOI: 10.15330/pcss.22.4.828-836

Vasyl Stefanyk Precarpathian National University

ФІЗИКА І ХІМІЯ ТВЕРДОГО ТІЛА
Т. 22, № 4 (2021) С. 828-836
Технічні науки

UDC 621.643:620.194.22 ISSN 1729-4428

L.I. Nyrkova, P.E. Lisovyi, L.V. Goncharenko, S.O. Osadchuk, V.A. Kostin, A.V. Klymenko

Regularities of Stress-Corrosion Cracking of Pipe Steel 09G2S at Cathodic Polarization in a Model Soil Environment

E.O. Paton Electric Welding Institute of the National Academy of Sciences of Ukraine, Kyiv, lnyrkova@gmail.com

Peculiarities of corrosion-mechanical fracture of 09G2S pipe steel samples in the conditions of cathodic protection were investigated. It was established that depending on the level of protective potential, stress-corrosion cracking of pipe steel of a ferrite-pearlite class 09G2S can occur by different mechanisms. The range of protective potentials was determined, at which the anodic dissolution and hydrogen embrittlement occur simultaneously during the fracture of steel, namely from -0.85 V to -1.0 V. The existence of the above mechanisms is confirmed by the change in the strength and viscosity properties of the steel and the morphology of the fractures. For steels of other manufacturing technology and grades, these potential areas may differ.

Keywords: low-carbon steel 09G2S of pipe assortment, coefficients of properties degradation, slow rate deformation, potentiometry, stress-corrosion cracking, hydrogen embrittlement, local anodic dissolution.

Received 26 August 2021; Accepted 28 December 2021.

Introduction

Today, underground pipelines are one of the most efficient ways to transport gas and oil. Corrosion insulation and electrochemical protection are used to protect them from the negative effects of the environment. However, it is almost impossible to achieve full protection, and after prolonged operation, the destruction of pipes still occurs [1, 2].

Long-term operation of pipelines contributes to the development of various types of damage [3-10], in particular: damage of protective covers [4, 5], corrosion damage to the pipe wall [6-10], the formation of defects in metal pipes of various origins (potholes, branched cracks, cracks in welds and seam area) [3]. According to the analysis of statistical data made by various experts, the main causes of gas pipelines accidents are slightly different, but the share of failures caused by corrosion, including stress-corrosion cracking, is from 20 to 40% [9-10].

Accidents that occur during the operation of pipelines significantly affect the ecological state of the environment [1-3, 11-12]. SCC is especially common on pipelines with polyethylene tape [4, 6, 13, 14]. Studies of stress-corrosion cracking of gas pipelines have been conducted for more than five decades, after the first recorded case in 1965 [1, 15].

Depending on the operating conditions and composition of the soil electrolyte, there are two main types of corrosion cracking of tubular steels – «classical», intergranular cracking in carbonate electrolytes with high pH values and «non-classical», transcrystalline cracking in dilute electrolytes with near neutral pH. Near neutral pH SCC is typical for Ukrainian gas pipelines.

In general, SCC at near neutral pH occurs at a corrosion potential of -760 to -790 mV (relative to the copper sulfate reference electrode, m.s.e.) under a peeling coating, where cathodic polarization is not achieved due to the shielding effect of the coating or some other factor of the pipe surface. The cracks are mostly transcrystalline, usually wide with significant corrosion of the crack edges. The coated electrolyte is a dilute solution of HCO_3 with a pH in the range from 5.5 to 7.5 [6, 16-18].

This type of SCC differs significantly from the

relatively well-studied SCC at high pH, which develops in a carbonate/bicarbonate medium with a pH of 9 to 13 at a potential of -600 to -750 mV (relative to m.s.e.). Cathodic protection is effective to provide such potentials. Cracks in this type of SCC are intergranular and narrow [6, 21, 22].

A number of works are devoted to the study of operational degradation of structural steels, which emphasizes a significant reduction in mechanical properties and characteristics of brittle fracture and resistance to SCC [21-23]. In recent years, the literature presents the results of research on the effect of cathodic polarization on stress-corrosion cracking of pipe steels [24-27]. However, most of the data relate to controlled rolling steels, such as X70, X80, etc. It is of interest to investigate the effect of cathodic polarization on the corrosion cracking of pipe steels with a different structure, which are used on main pipelines, in particular long-term operation. It is probable that, depending on the microstructure, the regularities of SCC may differ, i.e. brittle fracture will develop in a different range of protective potentials than for the above-mentioned steels.

Based on the above, the study of the peculiarities of the development of stress-corrosion cracking of gas pipelines made of 09G2S steel with cathodic protection is of great practical importance.

The purpose of this work is to study the patterns of stress-corrosion cracking of pipe steel 09G2S, in conditions that mimic the operating conditions of main gas pipelines.

I. Materials and test techniques

The samples for investigations applying the slow strain rate method were cut from the sheets of a pipe steel 09G2S of 10 mm thickness across the rolled metal. The samples were manufactured according to the sketch (Fig. 1, a). The cross-sectional area of the working part of the samples in the initial state was 30 mm^2, the length of the working part was 42 mm. The samples were stretched in air and in the solution at a rate of 10^{-6} s^{-1} in the rupture machine AIMA-5-1.

The surface of the samples was cleaned mechanically using SiC sandpaper with the grit granularity 800, washed with distilled water, degreased with magnesium dioxide and dried in air. The tests were performed at a slow strain rate in accordance with ISO 7539-1 [28]. The samples were stretched in the rupture machine AIMA-5-1 at a rate of 10^{-6} s^{-1} in the NS4 solution at an open curcuit potential and at induced cathode potentials in the range from -0.75 V to -1.2 V. All potentials were measured against saturated silver chloride reference electrode. The scheme of the installation is shown in Fig. 2.

As the working electrode, a sample of steel was served, the auxiliary electrode was platinum and the reference electrode was saturated silver chloride electrode. During the tests, stress and elongation of the sample were controlled. The chemical composition of steel 09G2S and its mechanical properties are presented in Table 1, 2, respectively.

The hardness of the steel is approximately (160-170) HV_5. Non-metallic inclusions were evaluated on non-etched sections. The steel contains non-metallic inclusions in some areas, mainly in the form of brittle silicates and fine rounded oxides (Fig. 1, *b*).

As to the structure this steel belongs to a low-carbon, low-alloy, silicon-manganese steel of ferrite-pearlite class, Fig. 1, *c*. The structure of steel contains ferritic and pearlitic grains in the ratio of 70 and 30%, respectively. Ferrite grains correspond to the size number (6-7) (according to GOST 5639 [29]). A part of perlite is arranged in the form of bands.

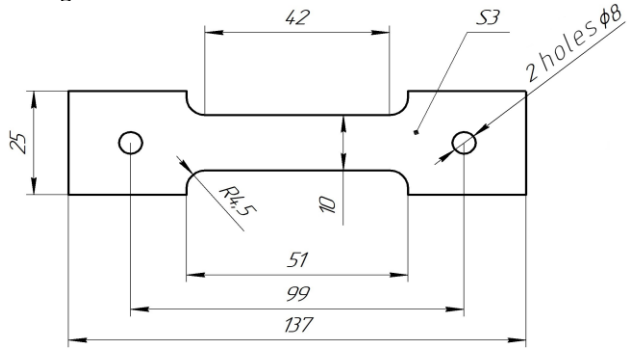

a)

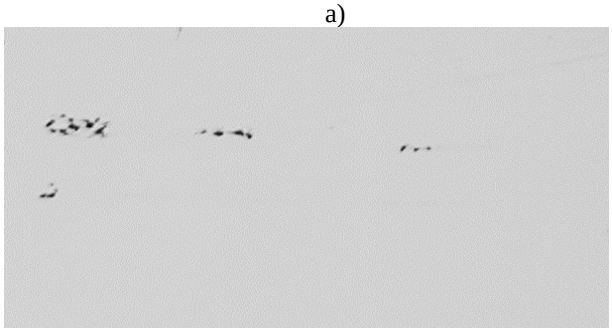

b)

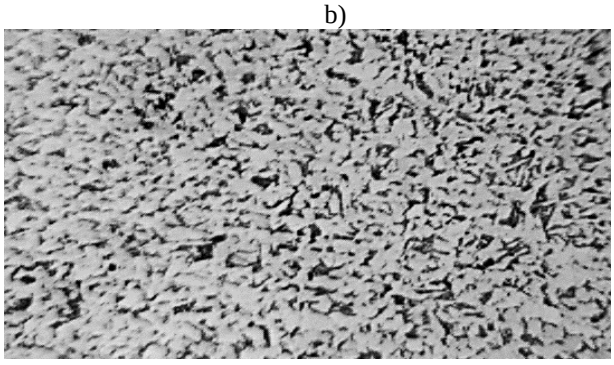

c)

Fig. 1. Sample for slow strain rate tests (a), non-metallic inclusions, ×50 (b) and microstructure of steel 09G2S, ×320 (c).

Table 1

Chemical composition of steel 09G2S.

Material	C	Mn	Si	S	P	Ni	V	Cr	Cu
Experimental sample	0.08	1.65	0.68	0.034	0.019	0.10	0.007	0.10	0.27
Steel 09G2S according to GOST 19282	0.12	1.3-1.7	0.5-0.8	0.035	0.03	0.25	0.12	0.3	0.3

Table 2

Mechanical properties of steel 09G2S

$\sigma_{0.2}$, MPa	σ_t, MPa	δ, %
325	470	21

To simulate a corrosive environment with a near-neutral pH, to which underground pipeline is exposed to, a neutral NS4 solution of the following chemical composition was used: 0,122 г/л KCl + 0,483 g/l $NaHCO_3$ + 0,181 г/л $CaCl_2$ + 0,131 г/л $MgSO_4$ (pH 8,2) [12, 18, 30-33]. Reagents of analytical grade and a distilled water were used. The tests were performed at a periodic wetting with a solution: 10 min in air and 50 min in the solution).

For testing in the conditions of periodic wetting the laboratory installation was developed, the sketch of which is presented in Fig. 2.

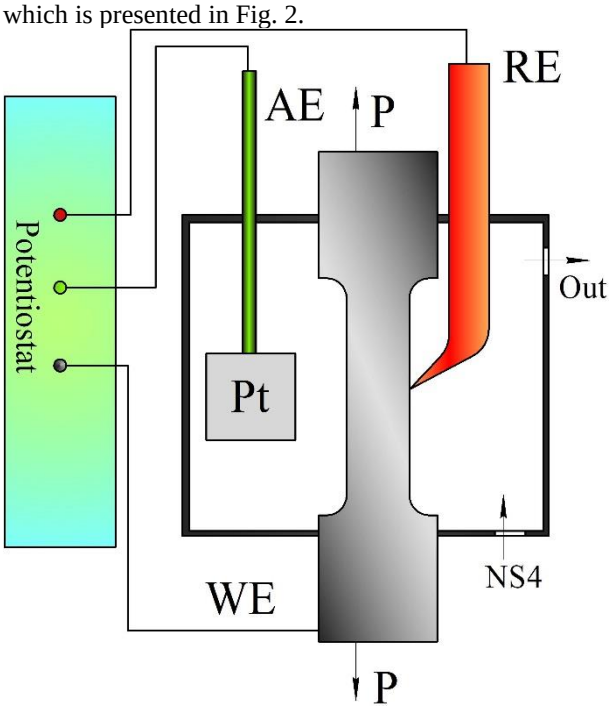

Fig. 2. Scheme of experimental installation for slow strain rate investigations. Designations: WE – working electrode, AE – auxiliary electrode, RE – reference electrode (saturated silver chloride).

Polarization curves were taken in the potentiodynamic mode according to the three-electrode scheme. Potentiostat PI-50-1.1, programmer PR-8 and recording device XY RECORDER A3 were used. The potential scanning rates were 0.5 and 100 mV/s depending on the purpose of the tests.

The degree of electrolytic hydrogenization of steel was determined applying the procedure according to GOST R 9.915 [35].

To study the microstructure, the method of optical microscopy was used. The sections were prepared according to the standard procedure. Detection of the structure was performed by etching in nital (4% solution of nitric acid in ethanol).

All the mechanical and electrochemical tests were performed at a room temperature under the conditions of free air access.

After rupture of the samples, their surface in the fracture zone and a fractography of the surface were analyzed. The surface of the fracture of the samples was cleaned by ultrasound and examined using a scanning electron microscope (SEM, Leica Cambridge Stereoscan S360, England).

II. Experimental results

2.1. Electrochemical tests

According to the model proposed in [35], in a corrosive environment, the edges of the crack during its propagation undergo the action of a cathodic polarization, and the tip may remain in an unbalanced state. Thus, the regularities according to which the process of stress-corrosion cracking of steel 09G2S proceeds in the conditions of a cathodic protection can be preliminarily evaluated by analyzing the polarization curves obtained at a high and a slow rate of potential scanning.

In Fig. 3 the potentiodynamic polarization curves of steel 09G2S in the NS4 solution obtained at a slow (0.5 mV/s) and a high (100 mV/s) potential scanning rates are presented. In the curves, the zone of active-passive transition is absent and the steel electrode was in the active state during the entire range of potentials both at a slow and a high polarization rates.

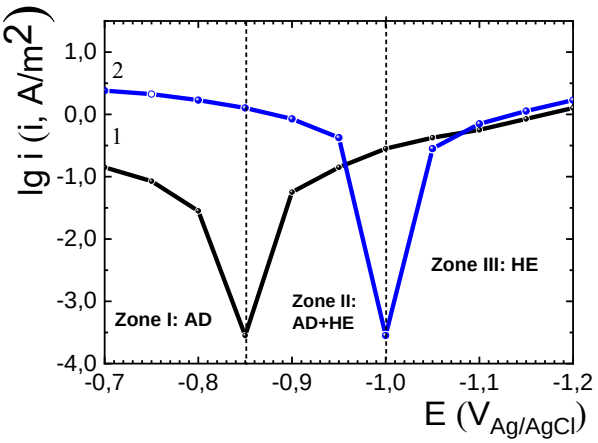

Fig. 3. Polarization curves of steel 09G2S at a potential scanning rate 0.5 mV/s and 100 mV/s.

The analysis of the polarization curves of steel 09G2S shows that the potential scanning rate has a significant effect on the corrosion potential: at a slow polarization, the corrosion potential becomes more positive due to a slower anodic dissolution, about -0.85 V, at a fast polarization it is more negative, -1.0 V. It was established that the position of the corrosion potential divides the range of potentials into three zones.

In the zone I, the anodic ionization reaction of iron is dominated

$$Fe \rightarrow Fe^{2+} + 2e^{-}, \quad (1)$$

in the zone III, the reactions of reduction of the aqueous electrolyte with the formation of hydrogen atoms occur:

$$O_2 + 2H_2O + 4e^{-} \rightarrow 4OH^{-} \quad (2)$$

$$H_2O + e^{-} \rightarrow H + OH^{-} \quad (3)$$

In the zone II, cathodic and anodic reactions can proceed simultaneously.

2.2. Slow strain rate test

The curves of corrosion-mechanical fracture of the samples are given in Fig. 4, *a*, tensile strength and elongation (b) of steel 09G2S at different potentials – in Fig. 4, *b*.

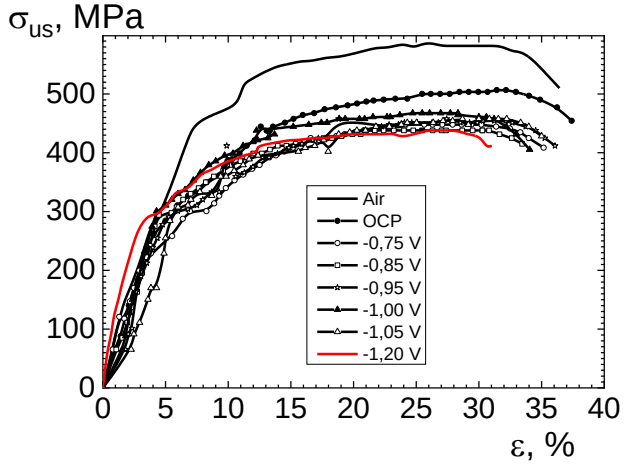

a)

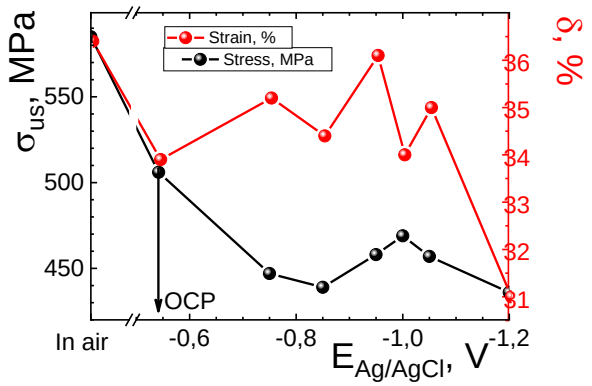

b)

Fig 4. Fracture diagrams (a), ultimate tensile strength and elongation (b) of steel 09G2S at different potentials.

Fig. 5 presents the picture of samples fracture area. It is obvious that under the action of the corrosive environment, the fracture of the samples occurs faster than in air, and a decrease in the ultimate tensile strength is noted.

Induction of a cathodic polarization accelerates the process of fracture, a significant decrease in strength (ultimate tensile strength) and ductility (elongation) is observed as compared to the similar indices during the tests in the solution at an OCP (open curcuit potential). As is follows from Fig. 4, b, the value of the tensile strength at an OCP and different cathode potentials is lower than in air. At the potential shifting from OCP to -0.85 V, a decrease in the tensile strength from 506 MPa to 440 MPa is noted, at a further potential shifting in the negative direction to -1.0 V – a slight increase to 450 MPa, and then – again a sharp decrease to 435 MPa are observed. The elongation of the samples at a cathodic polarization from -0.75 V to -1.05 V (corresponding to the range of protective potentials, normalized by DSTU 4219) varies within 2%, and at a potential of -1.2 V, it decreases to 31%, Fig. 3, b. The most intense decrease in the mechanical characteristics of the steel is observed at a potential of -1.2 V.

The obtained data are in agreement with the results of studies by other authors, which indicate that during the fracture of cathodic polarization, the tensile strength does not always change much, the elongation decreases more intensely [37]. The analysis of the area of fracture of the samples (Fig. 6) shows that with shifting of the potential to more negative values, the cross-sectional area increases.

On the samples that fractured in the solution at the potentials from OCP to -0.85 V, near the edge of the fracture, the signs of plastic deformation were detected. In some samples, short secondary cracks are visible, located parallel to the rupture line.

At the potentials from -0.85 to -1.0 V, on the surface of the samples, in addition to the signs of plastic deformation, deeper secondary cracks are visible, the number of which is greater than on the samples at more positive potentials. The shape of the edge of the rupture is more complex: in addition to smooth areas, step-like areas are observed.

At the potentials more negative than -1.0 V, the plastic deformation is much lower, the rupture line is complex broken and deep secondary cracks are present.

To analyze the sensitivity of steel 09G2S to SCC under the conditions of cathodic polarization, the coefficients of loss of tensile strength ($F\sigma_{us}$), cross-sectional area (F_S) and relative elongation (F_δ) were calculated. The change in mechanical properties in the solution was compared with the corresponding values in air:

$$F_{\sigma_{us}} = \left(1 - \frac{\sigma_{us}^{s}}{\sigma_{us}^{air}}\right) \times 100\% \quad (4)$$

$$F_S = \left(1 - \frac{S_s}{S_{air}}\right) \times 100\% \quad (5)$$

$$F_\delta = \left(1 - \frac{\delta_s}{\delta_{air}}\right) \times 100\% \quad (6)$$

σ_{us}^{s}, S_s, δ_s and σ_{us}^{air}, S_{air}, δ_{air} are the ultimate tensile strength, cross-sectional area and relative elongation of the samples in the solution and in air, respectively.

The degree of sensitivity to SCC was estimated also by the dimensionless coefficient K_S [36, 37], which was count as the ratio of the relative reduction in area of a specimen in air to the relative reduction in area in the solution according to the formula (7):

$$K_S = \frac{\psi_{air}}{\psi_S} \quad (7)$$

where ψ_{air} and ψ_S are the relative reduction in area of specimens, respectively, in air and in the solution.

Fig. 5. Photo of surfaces near the area of fracture samples at different potentials in the NS4 solution.

With shifting of the potential from OCP to more negative values in the zone I, all the coefficients change little, Fig. 7. In the zone II, a decrease in F_δ and a nonmonotonic change in $F_{\sigma us}$ and F_S are observed. In the zone III, the most significant loss of all properties of the steel is observed, namely: strength, elongation and cross section.

The coefficient of susceptibility to SCC in the zone I is in the range from 1.04 to 1.15, in the zone II, a tendency to its increase is observed, and in the zone III, it increases to 1.25 at the potentials from -1.05 V to -1.2 V.

Since F_S and F_δ are the coefficients of loss of ductility, then, at the induction of more negative potentials, the sensitivity to SCC increases. However, when the potential is shifted in the cathode direction to -1.05 V, a significant change in $F\sigma_B$ is not observed, an increase in the loss of strength to almost 15% was established only at more negative potentials. Therefore, the susceptibility of steel 09G2S to SCC has a complex dependence on the induced cathode potential.

2.3 Nature of fracture surface during corrosion and mechanical tests

The morphology of fracture surfaces under the conditions of cathodic polarization in the NS4 solution is presented in Fig. 6.

Microscopic analysis of the fracture surface showed that the fracture occurs by a different mechanism.

During fracture in air, the fracture surface of the sample has a ductile dimple morphology. The fracture occurs by a ductile type (Fig. 6, in air).

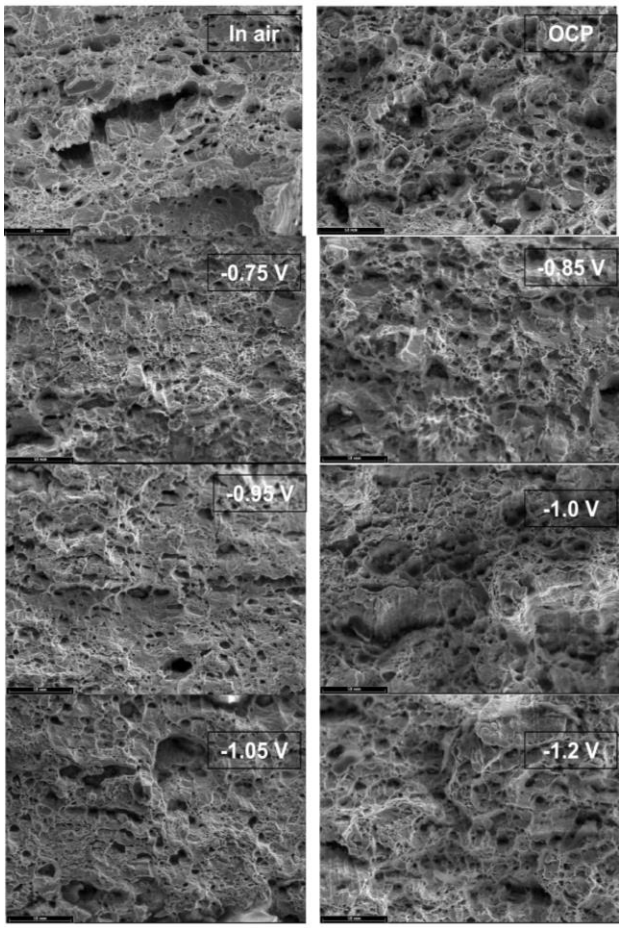

Fig. 6. Morphology of fracture surfaces of samples under the conditions of cathodic polarization in the NS4 solution.

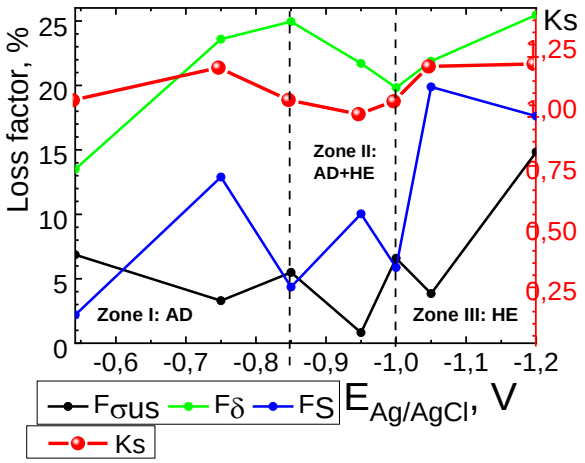

Fig. 7. Coefficients of loss of properties of steel 09G2S during corrosion-mechanical tests and change in the coefficient of susceptibility to SCC at a cathodic polarization in the NS4 solution.

At the potentials, more positive than -0.85 V (Fig. 6, photo at the OCP and at the potential -0,75 V), on the fracture surface mostly ductile plastic structure with a large number of fracture dimples is formed, which indicates a low sensitivity of these samples to stress-corrosion cracking.

An increase in the cathodic polarization potential from -0.85 V to -1.0 V leads to an increase in the fraction of a brittle failure in the fracture, while the fraction of the plastic component decreases with an increase in the size of dimples and their depth (Fig. 6, photo at the potentials -0.85 V, -0,95 and -1,0 V). Analysis of fractures shows an increase in the varied grain sizes of dimples in the fracture: along with large dimples (not more than 10-15 μm) finer (not more than 1 μm) were detected, which are concentrated at the boundaries around the large dimples. It is probably, that smaller dimples were formed at the final stage of stress-corrosion fracture. In addition, for this zone of potentials, on the fractograms of the fracture surfaces, facets of chipping and delamination of the metal were revealed, which are the signs of an increased susceptibility of the metal to brittle fracture.

At the potentials greater than -1.0 V (Fig. 6, photo at the potentials -1.05 and -1,2 V), the fraction of dimple fracture and the depth of dimples is much smaller, an increase in the share of chip and delamination surfaces is observed. This type of fracture surface is characteristic of hydrogen-induced fracture, demonstrated by [27-29].

III. Discussion

During stress-corrosion cracking, a fresh metal surface is formed at the crack tip, so the crack tip remains always in an unbalanced state of electrochemical reaction. On the edges of the crack, corrosion products are formed, under which the electrochemical reaction of iron ionization occurs (1). Having considered the electrochemical state at the tip and at the edges of the crack, it is possible to obtain data on the SCC mechanism.

With the help of polarization curves at a fast and a slow potential scanning rate, it is possible to simulate the conditions, created at the tip of the crack and at its edges, respectively. Depending on the induced cathode potential, at the tip and at the edges of the crack different electrochemical reactions proceed. At a slow potential scanning rate, the steel is in a quasi-equilibrium state. When this equilibrium is disturbed by polarization, the cathode reaction occurs at a more negative potential due to shifting of the corrosion potential to more negative values. At a high rate of polarization, the steel reaches another quasi-equilibrium state, at which a new stationary polarization is established. Thus, a high potential scanning rate indicates areas where an intense anode activity exists, while a relatively slow potential change rate will indicate areas where relative stability is probable [37].

In the zone I (potentials, which are more positive than -0.85 V), both the tip of the crack as well as its edges are subjected to anodic dissolution according to the reaction (1). The fracture of the samples at these potentials was accompanied by a plastic deformation, the values of K_S were low – from 1.04 to 1.15, the morphology of a fracture had mostly a ductile dimple nature. It is probably, that the concentration of hydrogen atoms formed at this level of polarization is quite low, Fig. 7, and the formed hydrogen does not participate in the process of fracture. In this range of potentials, the process of stress-corrosion cracking proceeds by the mechanism of a local anodic dissolution.

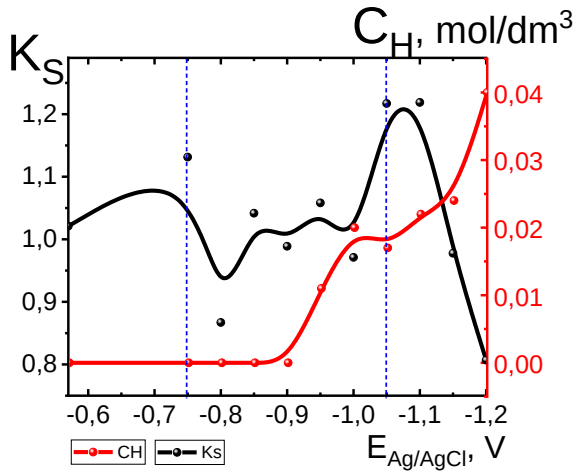

Fig. 8. Coefficient of susceptibility to corrosion cracking and concentration of hydrogen, which penetrates steel 09G2S at cathodic polarization.

In the zone of potentials II (from -0.85 V to -1.0 V), as follows from the polarization curves, the crack tip remains still in the state of anodic dissolution, while its edges undergo the action of cathodic polarization. On the samples near the rupture line, except for the signs of plastic deformation, deep secondary cracks are visible. For this zone, a nonmonotonic change in the coefficients of fracture $F\sigma_B$, F_S and F_δ is characterized, a tendency to increase the coefficient of susceptibility to SCC – K_S is noted. In the fractures, dimples of different sizes and depths and fragments of chips and delamination surfaces are formed. At the potentials from -0.85 V to -1.0 V, the concentration of reduced hydrogen increases, Fig. 7, and an opportunity for its penetration into the metal under the action of tensile stresses is created. The mixed ductile-brittle fracture morphology and nonmonotonic change in the values of mechanical properties indicate a mixed mechanism of stress-corrosion cracking. And depending on the direction, in which its equilibrium is shifted, the fraction of brittle and ductile components in the morphology of the fracture surface varies.

In the zone of potentials III (more negative than -1.0 V), the fracture occurs almost without plastic deformation, but on the surface near the line of fracture, many secondary cracks of different lengths are formed.

On the surface of the fracture, the fraction of chips and delamination facets increases and an increase in the coefficients of loss of such mechanical properties: strength, elongation, cross section and the coefficient of susceptibility to SCC to 1.25 is observed. At the potentials more negative than -1.0 V, an active reduction of hydrogen occurs, its concentration in steel increases quite sharply, Fig. 7, and it is actively involved in the process of fracture. Namely, at such potentials, an increase in the susceptibility of steels to brittle fracture is observed. In this range of potentials, the process of stress-corrosion cracking occurs by a hydrogen mechanism.

Conclusions

The mechanism of propagation of stress-corrosion cracking of pipe steel 09G2S in the model soil environment was investigated. It was established that the SCC mechanism varies depending on the induced polarization potential. At a low cathode potential, positively than -0,85 V, the predominant mechanism of SCC is a local anodic dissolution and at a high potential, negatively than -1,0 V, the the dominant mechanism is a hydrogen embrittlement. Also an intermediate range of potentials (from -0.85 V to -1.0 V) exists, in which the anodic dissolution occurs simultaneously with the hydrogen embrittlement. The change in the mechanism of stress-corrosion cracking is confirmed by the change in the strength and ductile properties of steel, susceptibility to brittle cracking, increasing of the hydrogen penetration into steel and the morphology of sample fractures.

Acknowledgement

The work was carried out within the framework of the departmental order program of the National Academy of Sciences of Ukraine by the E.O. Paton Electric Welding Institute in 2019-2021 (fundamental research works) "Improving the operational reliability of main pipelines and oil storage tanks by providing technological guarantees for the quality of welded joints and optimizing the conditions of their safe operation" (State registration number 0118U100537).

Nyrkova L.I. – Doctor of technical sciences, Head of the Department of welding of gas and oil pipelines;
Lisovyi P.E. – PhD student of the Department of welding of gas and oil pipelines,
Goncharenko L. V. – Junior researcher of Department welding of gas and oil pipelines;
Osadchuk S.O. – PhD in technical sciences, Researcher of the Department of welding of gas and oil pipelines;
Kostin V. A. – Doctor of technical sciences, Leading Researcher of the Department of physico-chemical studies of materials;
Klymenko A. V. – PhD in technical sciences, Senior Researcher of the Department of gas and oil welding.

[1] A. Ya. Krasovskii, I. V. Lokhman, I.V. Orynyak. Strength of Materials 44 (2), 129 (2012), https://doi.org/10.1007/s11223-012-9366-5.
[2] National Energy Board, Report of Public Inquiry concerning Stress Corrosion Cracking on Canadian Oil and Gas Pipelines, MH-2-95, November (1996).
[3] L. Poberezhny, A. Yavorsky, V. Tsyh, A. Stanetsky, A. Grytsanchuk, Scientific and technical journal «Technogenic and ecological safety» 1, 24 (2017).

[4] M Roche. The problematic of disbonding of coatings and corrosion with buried pipelines cathodically protected in: EFC WP16, 10th meeting, EUROCORR'2004, Nice, Sept. 14, 2004.
[5] D. Melot, Paugam, G., Roche, M. Journal of Protective Coatings & Linings, pp. 18-31, 2009 (https://www.paintsquare.com/library/articles/Disbondments_of_Pipeline_Coatings_and_Their_Effects_on_Corrosion_Risks.pdf)
[6] R. N. Parkins, W. K. Blanchard, B.S. Delanty. Corrosion 50(5), 394 (1994), https://doi.org/10.5006/1.3294348.
[7] J.B. Choi, B.K. Goo, J.C Kim, Y.J. Kim, W.S.Kim, International Journal of Pressure Vessels and Piping 80(2), 121 (2003), https://doi.org/10.1016/S0308-0161(03)00005-X.
[8] K.J. Yeom, Y.K. Lee, K.H. Oh, W.S. Kim, Engineering Failure Analysis, 57, 553 (2015), https://doi.org/10.1016/j.engfailanal.2015.07.024.
[9] V. Khrutba, G Weigang, O. Stegniy, Ecological safety, 24 (2), 75 (2017).
[10] R.I. Bogdanov, I.V. Ryakhovskyh, Scientific and practical youth seminar, vil. Razvilka, Moscow distr., 15 –16 of Apryl, 2015.
[11] J.A. Beavers, G. Neil, External Corrosion of Oil and Natural Gas Pipelines. ASM Handbook, 13C, Corrosion: Environments and Industries (№ 05145), Corrosion in Specific Industries, 1015.
[12] B. Fang, A. Atrens, J. Wang, E.Z.Han Zhu, W. Ke, Journal of Materials Science 38, 127 (2003), https://doi.org/10.1023/A:1021126202539.
[13] R.L Wenk, 5th Symp. On Line Pipe Research, Catalog No. L30174 (American Gas Association, Arlington, VA, 1974, T-1.
[14] Eslami A., B. Fang, R. Kania, B. Worthingham, J. Been, R. Eadie, W. Chen, Corrosion Science, 52, 3750 (2010), https://doi.org/10.1016/j.corsci.2010.07.025Get rights and content.
[15] B.S. Delanty, J. O'Beirne, Oil Gas Journal, 15, 39 (1992).
[16] S. Wang, W. Chen, F. King:, Corrosion, 58 (6), 526 (2002), https://doi.org/10.5006/1.3277644.
[17] R. Chu, W. Chen, S.H. Wang, F. King, T.R. Jack, R.R. Fessler, Corrosion, 60(3), 275 (2004), https://doi.org/10.5006/1.3287732.
[18] L. Niu, Y.F. Cheng, Applied surface science, 253(21), 8626 (2007), https://doi.org/10.1016/j.apsusc.2007.04.066.
[19] F.M. Song, Corrosion science, 51(11), 2657 (2009), https://doi.org/10.1016/j.corsci.2009.06.051.
[20] J.Q. Wang, A. Atrens, Corrosion Science, 45(10), 2199 (2003), https://doi.org/10.1016/S0010-938X(03)00044-1.
[21] L. Poberezhnyi, P. Maruschak, O. Prentkovskis, I. Danyliuk, T. Pyrig, J. Brezinová. Archives of Civil and Mechanical Engineering, 16(3), 524-536 (2016), https://doi.org/10.1016/j.acme.2016.03.003.
[22] T. Vilkys, V. Rudzinskas, O. Prentkovskis, J. Tretjakovas, N. Višniakov, P. Maruschak, *Metals 8*(5), 346 (2018), https://doi.org/10.3390/met8050346.
[23] M. Chausov, P. Maruschak, A. Pylypenko., A. Sorochak In *Degradation Assessment and Failure Prevention of Pipeline Systems*, 189 (2021), https://link.springer.com/chapter/10.1007/978-3-030-58073-5_15.
[24] R. Galván-Martínez, R.Orozco-Cruz, A. Carmona-Hernández, E. Mejía-Sánchez, M. A Morales-Cabrera, A. Contreras, Metals, 9(12), 1 (2019), https://doi.org/10.3390/met9121353.
[25] Z.Y. Liua, X.G. Li, Y.F. Cheng, Electrochimica Acta, 60(15), 259 (2012), https://doi.org/10.1016/j.electacta.2011.11.051.
[26] S.C. Silva, A.B. Silva, M.C. Folena, R. Barker, A. Neville, J.P. Gomes, Engineering Failure Analysis, 104550, (2020), https://doi.org/10.1016/j.engfailanal.2020.104550.
[27] J. Capelle, J. Gilgert, I. Dmytrakh, G. Pluvinage, International journal of hydrogen energy, 33(24), 7630 (2008), https://doi.org/10.1016/j.ijhydene.2008.09.020.
[28] [28] Corrosion of metals and alloys — Stress corrosion testing — Part 1: General guidance on testing procedures. ISO 7539-1:2012.
[29] Steel and alloys. Methods for detection and determination of grain size. GOST 5639-82.
[30] R Antunes de Sena, I. Napoleão Bastos, G. Mendes Platt, International Scholarly Research Notices. Article ID 103715, 6 pages, (2012).
[31] B. Gu, J. L. Luo, W.Z. Mao, X. Yu, Corrosion, 55 (3), 312 (1999), https://doi.org/10.5006/1.3283993.
[32] T.M. Ahmed, S.B. Lambert, A. Plumtree, R. Sutherby, Corrosion, 53(7), 581 (1997), https://doi.org/10.5006/1.3290290.
[33] B. Gu, J. Luo, X. Mao, Corrosion, 55(1) 96 (1999), https://doi.org/10.5006/1.3283971.
[34] Unified system of corrosion and ageing protection. Metals, alloys, coatings, products. Test methods of hydrogen embrittlement. GOST R 9.915-2010.
[35] Z.Y. Liu, X.G. Li, Y.F. Cheng, Corrosion Science, 55, 54 (2012), https://doi.org/10.1016/j.corsci.2011.10.002.
[36] L. Nyrkova, Engineering Failure Analysis, 116, 104757 (2020), https://doi.org/10.1016/j.engfailanal.2020.104757.
[37] L.I. Nyrkova, S.O. Osadchuk, A.O. Rybakov, S.L. Mel'nychuk, Materials Science, 55, 625 (2020), https://doi.org/10.1007/s11003-020-00352-x.

Л.І. Ниркова, П.Є. Лісовий, Л.В. Гончаренко, С.О. Осадчук, В.А. Костін, А..В.Клименко

Закономірності стрес-корозійного розтріскування трубної сталі 09Г2С при катодній поляризації в модельному ґрунтовому середовищі

Інститут електрозварювання імені Є.О. Патона НАН України,Київ, lnyrkova@gmail.com

Досліджено особливості корозійно-механічного руйнування зразків труби 09Г2С в умовах катодного захисту. Встановлено, що в залежності від рівня захисного потенціалу, корозійно-корозійне розтріскування трубної сталі феритно-перлітового класу 09Г2С може відбуватися різними механізмами. Визначено діапазон захисних потенціалів, при якому анодне розчинення та водневе окрихчення відбуваються одночасно під час руйнування сталі, а саме від -0,85 В до -1,0 В. Наявність вищезазначених механізмів підтверджується зміною міцності та в'язкостних властивостей сталі та морфологією руйнування. Для сталей інших технологій виробництва та марок ці області потенціалів можуть відрізнятися.

Ключові слова: низьковуглецева сталь 09Г2С сортименту труб, коефіцієнти деградації властивостей, повільна деформація, потенціометрія, напружено-корозійне розтріскування, воднева окрихкість, локальне анодне розчинення.